Biochemical Pharmacology 80 (2010) 1632–1640

Contents lists available at ScienceDirect

Biochemical Pharmacology

journal homepage: www.elsevier.com/locate/biochempharm

Activation of ceramide synthase 6 by celecoxib leads to a selective induction of $C_{16:0}$-ceramide

Susanne Schiffmann *, Simone Ziebell, Jessica Sandner, Kerstin Birod, Klaus Deckmann, Daniela Hartmann, Sina Rode, Helmut Schmidt, Carlo Angioni, Gerd Geisslinger, Sabine Grösch

pharmazentrum frankfurt/ZAFES, Institut für Klinische Pharmakologie, Klinikum der Goethe-Universität Frankfurt, Theodor-Stern-Kai 7, 60590 Frankfurt/Main, Germany

ARTICLE INFO

Article history:
Received 28 June 2010
Accepted 13 August 2010

Keywords:
Cancer
Cyclooxygenase-2
(Dihydro)ceramide synthase
$C_{16:0}$-ceramide
Celecoxib
siRNA

ABSTRACT

Ceramides serve as bioactive molecules with important roles in cell proliferation and apoptosis. Ceramides (Cer) with different N-acyl side chains ($C_{14:0}$-Cer–$C_{26:0}$-Cer) possess distinctive roles in cell signaling and are differentially expressed in HCT-116 colon cancer cells. Celecoxib, a selective cyclooxygenase-2 (COX-2) inhibitor, exhibiting antiproliferative effects, activates the sphingolipid pathway. To elucidate the mechanism, HCT-116 cells were treated with 50 μM celecoxib leading to a significant increase of $C_{16:0}$-Cer. Interestingly, 50 μM celecoxib resulted in a 2.8-fold increase of ceramide synthase (CerS) activity as measured by a cell-based activity assay. siRNA against several CerSs revealed that CerS6 was predominantly responsible for the increase of $C_{16:0}$-Cer in HCT-116 cells. Moreover, the silencing of CerS6 partially protected HCT-116 cells from the toxic effects induced by celecoxib. Treatment of cells with celecoxib and fumonisin B1 (inhibitor of CerSs) or myriocin (inhibitor of L-serine palmitoyl transferase) or desipramine (inhibitor of acid sphingomyelinase and acid ceramidase) revealed that the increase of $C_{16:0}$-Cer results predominantly from activation of the salvage pathway. Using the nude mouse model we demonstrated that celecoxib induces also *in vivo* a significant increase of $C_{16:0}$-Cer in stomach, small intestine and tumor tissue. In conclusion, celecoxib causes a specific increase of $C_{16:0}$-Cer by activating CerS6 and the salvage pathway, which contribute to the toxic effects of celecoxib.

1. Introduction

As the backbone of several complex sphingolipids (sphingomyelins, glycosylceramides), ceramides are members of the rapidly expanding field of bioactive lipids, which play important roles in the regulation of cell growth, cell differentiation, apoptosis and cell senescence [1]. Briefly, ceramides are synthesized *de novo* from L-serine and palmitoyl-CoA, which are converted subsequently by L-serine palmitoyl transferase (SPT) and 3-ketosphinganine reductase to sphinganine. Acyl-CoAs with chain lengths between C_{14} and C_{26} are attached to sphinganine by chain length specific (dihydro)ceramide synthases (CerS1-6) [2] to form C_{14}–C_{26}-dihydroceramides. Dihydroceramide desaturase converts these intermediates to C_{14}–C_{26}-ceramides. Sphingosine, produced by the salvage pathway, is also accepted by these CerSs as a substrate, leading to the synthesis of C_{14}–C_{26}-ceramides without the intermediate dihydroceramide (Fig. 1A). In some tissues such as the testes, ceramides of lengths up to C_{32} have been detected [3]. As an alternative to *de novo* synthesis, complex sphingolipids may be degraded to ceramides and subsequently to sphingosine in the lysosome as part of the salvage pathway (Fig. 1A).

The CerS isoforms differ in their substrate specificities and their tissue distribution. Recent publications [4–7] on substrate specificity using cell culture experiments assigned the CerS isoforms to various N-acyl side chains starting with the short chain ceramides as follows: CerS5 ($C_{16:0}$-Cer, $C_{18:0}$-Cer, $C_{18:1}$-Cer); CerS6 ($C_{16:0}$-Cer, $C_{18:0}$-Cer); CerS1 ($C_{18:0}$-Cer); CerS3 ($C_{18:0}$-Cer, $C_{20:0}$-Cer); CerS4 ($C_{18:0}$-Cer, $C_{20:0}$-Cer, $C_{22:0}$-Cer, $C_{24:0}$-Cer); CerS2 ($C_{20:0}$-Cer, $C_{22:0}$-Cer, $C_{24:0}$-Cer). These data indicate a substantial degree of overlap in substrate specificity among the isoforms, obscuring assignment of a specific ceramide to a specific CerS isoform.

Ceramides exhibit antiproliferative and proapoptotic effects [8]. Several chemotherapeutics are known to induce apoptosis and/or inhibit cell growth via generation and accumulation of ceramides, either via activation of *de novo* synthesis or through the salvage pathway by the hydrolysis of sphingomyeli-

Abbreviations: Cer, ceramide; COX-2, cyclooxygenase-2; dhCer, dihydroceramide; CerS, (dihydro)ceramide synthase; DES, dihydroceramide desaturase; FB1, fumonisin B1; GCS, glucosylceramide synthase; KSR, 3-ketosphinganine reductase; Myr, myriocin; SMS, sphingomyelin synthase; SMase, sphingomyelinase; Sph1P, sphingosine-1-phosphate; Sph1PP, sphingosine-1-phosphate phosphatase; dhSph, sphinganine; dhSph1P, sphinganine-1-phosphate; SPT, L-serine palmitoyl transferase.

* Corresponding author. Tel.: +49 69 6301 7820; fax: +49 69 6301 7636.
E-mail address: susanne.schiffmann@med.uni-frankfurt.de (S. Schiffmann).

0006-2952/$ – see front matter © 2010 Elsevier Inc. All rights reserved.
doi:10.1016/j.bcp.2010.08.012

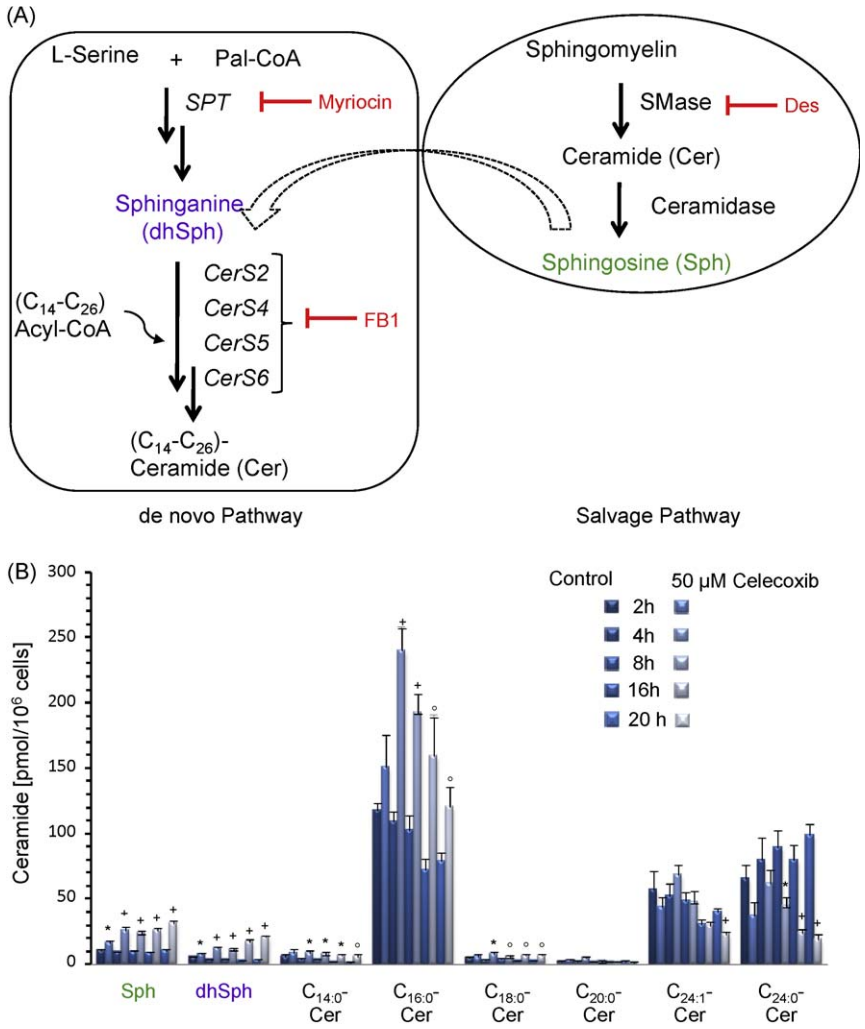

Fig. 1. (A) Scheme of the sphingolipid *de novo* synthesis and the salvage pathway. SPT, L-serine palmitoyltransferase; Myr, myriocin; CerS, (dihydro)ceramide synthase; FB1, fumonisin B1; SMase, sphingomyelinase, Des, desipramine. (B) Time-dependent alteration of the sphingolipid level in HCT-116 cells treated with celecoxib. The cells were treated for various time points (2 h, 6 h, 8 h, 16 h, 20 h) with 50 μM celecoxib (light blue) or with DMSO (control, dark blue). The ceramide levels were determined with LC–MS/MS and normalized to the number of treated cells. Data are mean ± S.E.M. of two independent experiments each achieved in triplicate. $^{*}p < 0.05$, $^{\circ}p < 0.01$, $^{+}p < 0.001$ indicate significant difference between celecoxib and DMSO-treated cells at the various time points.

nases (SMase) [9,10]. Which of these pathways are activated depends on the cell type and stimulus (for review see [11]). Interestingly, there are early data suggesting that cancer cells, but not normal cells, are hyper-sensitive to ceramides, thereby raising the sphingolipid pathway as a possible target for cancer therapy [12,13].

Celecoxib, a selective COX-2 inhibitor, exhibits proapoptotic and growth inhibiting effects in various cancer cells and animal tumor models [14]. It is approved for the adjuvant treatment of familial adenomatous polyposis, an inherited syndrome that predisposes individuals to colon cancer [15]. The antiproliferative activity of celecoxib correlates with inhibition of COX-2 as well as with its ability to inhibit non-COX-2 targets such as 3-phosphoinositide-dependent protein kinase-1 (PDK1), sarcoplasmic/endoplasmic reticulum calcium ATPase (SERCA) [16] and 5-lipoxygenase [17].

A previous study from our group demonstrated that celecoxib influences the sphingolipid pathway by inhibiting dihydroceramide desaturase with an IC_{50} of 79 μM [18]. In addition to a specific decrease of $C_{24:0}$-Cer/$C_{24:1}$-Cer concentration and an increase of dihydroceramide concentration, we also observed an elevation of total ceramide (ceramides and dihydroceramides) levels, which were causatively linked to the apoptotic and growth inhibiting properties of celecoxib. This increase in total ceramide levels after celecoxib treatment cannot exclusively be explained by inhibition of the dihydroceramide desaturase. Therefore, we looked for further targets in the sphingolipid pathway that also could be influenced by celecoxib and thereby contribute to the observed changes in the sphingolipid levels in HCT-116 cells.

2. Experimental

2.1. Cells and reagents

The human cancer cell line HCT-116 was ordered from Deutsche Sammlung für Mikroorganismen und Zellkulturen (DSMZ, Braunschweig, Germany). HCT-116 cells were incubated in McCoy's 5A supplemented with 100 units/ml penicillin G, 100 μg/ml streptomycin, 10% FCS (fetal calf serum) for culturing and 7.5% FCS in case of treatment. Cells were cultured at 37 °C in an atmosphere containing 5% CO_2. Myriocin, fumonisin B1 and desipramine were purchased from Sigma–Aldrich (Schnelldorf, Germany). siRNAs (CerS2 (s26788), CerS4 (s35896), CerS5 (s40552), CerS6 (s48449)) were purchased from Ambion (Darmstadt, Germany). The sphingolipids and palmitoyl-CoA were purchased

either from Avanti Polar Lipids (Alabaster, USA) or Matreya LLC (Pleasant Gap, USA). Celecoxib was synthesized by WITEGA Laboratorien Berlin-Adlershof GmbH. The identity and purity of celecoxib was determined using ^{1H}NMR (nuclear magnetic resonance) spectroscopy and high performance liquid chromatography (HPLC) as described previously [19] and was >99%.

2.2. Determination of sphingolipid concentrations in cells and in mouse tissue

For the quantification of sphingolipid amounts, cells were seeded at a density of 0.5×10^6/5 cm dish and incubated for 24 h. Subsequently, cells were treated with celecoxib in the presence or the absence of 150 nM myriocin and/or 5 μM sphingosine(C_{17}) over various periods of time. The sphingolipids were extracted with methanol as previously described [18]. The mouse tissue was homogenated in PBS and extracted with a mixture of chloroform/methanol (7:1). The extraction and the determination of the sphingolipid concentrations ($C_{16:0}$-Cer, $C_{18:0}$-Cer, $C_{20:0}$-Cer, $C_{24:1}$-Cer, $C_{24:0}$-Cer, $C_{16:0}$-dhCer, $C_{24:1}$-dhCer, $C_{24:0}$-dhCer, dhSph, Sph) by liquid chromatography coupled to tandem mass spectrometry (LC–MS/MS) was achieved as published previously [18,20]. Ceramides labeled by the introduction of Sph(C_{17}) exhibit precursor-to-product ion transitions of m/z 496 → 250 for $C_{14:0}$-Cer(C_{17}), of m/z 524 → 250 for $C_{16:0}$-Cer(C_{17}), of m/z 552 → 250 for $C_{18:0}$-Cer(C_{17}), of m/z 580 → 250 for $C_{20:0}$-Cer(C_{17}), of m/z 608 → 250 for $C_{22:0}$-Cer(C_{17}), of m/z 634 → 250 for $C_{24:1}$-Cer(C_{17}), of m/z 636 → 250 for $C_{24:0}$-Cer(C_{17}), of m/z 662 → 250 for $C_{26:0}$-Cer(C_{17}), of m/z 552 → 534 for $C_{17:0}$-Cer and of m/z 286 → 268 for Sph(C_{17}), which were used for the Multiple Reaction Monitoring with a dwell time of 15 ms. For analysis, the area under the peak of the analyte was related to the area under the peak of the internal standard. The relative increase of the specific ceramides was calculated using the ratio of analyte to internal standard of untreated cells as the value of 100%. Data were normalized to the number of treated cells.

2.3. Determination of palmitoyl-CoA concentrations in cells

For the quantification of palmitoyl-CoA ($C_{16:0}$-CoA) amounts, cells were seeded at a density of 0.5×10^6, incubated for 24 h and incubated with 50 μM celecoxib for various times. Lipids were extracted with 125 μl acetonitrile/water (50:50, v/v) after the addition of the internal standard ($C_{17:0}$-CoA). The suspension was sonicated on ice, thoroughly mixed for 1 min and centrifuged for 3 min at 25 °C and 20,500 × g. The supernatants were collected and the extraction step (no sonication) was repeated with 100 μl acetonitrile/water (50:50, v/v). The amounts of $C_{16:0}$-CoA and the internal standard were determined by LC–MS/MS. Chromatographic separation was accomplished under gradient conditions using a Gemini C18 column (150 mm × 2 mm ID, 5 μm particle size; Phenomenex, Aschaffenburg, Germany). The HPLC mobile phases consisted of water/ammonium hydroxide (100:0.5, v/v) (A) and acetonitrile/ammonium hydroxide (100:0.5, v/v) (B). MS/MS analyses were performed on an API 5500 triple quadrupole mass spectrometer with a Turbo V source (Applied Biosystems, Darmstadt, Germany) in the negative ion mode. Precursor-to-product ion transitions of m/z 501.7 → 78.9 for $C_{16:0}$-CoA and of m/z 508.6 → 78.9 for $C_{17:0}$-CoA were used for the MRM with a dwell time of 200 ms. Concentrations of the calibration standards, quality controls and unknowns were evaluated by Analyst software version 1.5 (Applied Biosystems). Linearity of the calibration curve was proven from 1 ng/ml (0.94 pmol/ml) to 100 ng/ml (94 pmol/ml). The coefficient of correlation for all measured sequences was at least 0.99.

2.4. Determination of mRNA and protein level of CerSs in cells

The mRNA was isolated using an RNA isolation kit (Qiagen, Hilden, Germany) according to the manufacturer's instructions. cDNA synthesis from 200 ng mRNA was performed using random hexamers of the verso cDNA Kit (Thermo Scientific, Dreieich, Germany). The expression levels of CerS1-6 and SPT were determined by Taqman™ analysis using the SYBR Green Kit (ABgene Limited, Epsom, United Kingdom) with an ABI Prism 7500 Sequence Detection System (Applied Biosystems, Austin, USA). Relative expression of SPTLC2 and CerS family genes was determined using the comparative CT (cycle threshold) method, normalizing relative values to the expression level of β-actin as a housekeeping gene. The designed primer sets were published previously [20]. Linearity of the assays was determined by serial dilutions of the templates for each primer set separately. For western blot analysis the CerS2, CerS6 and HSP90 antibody were purchased from Santa Cruz (Heidelberg, Germany), Sigma–Aldrich (Schnelldorf, Germany) and BD Bioscience (Heidelberg, Germany), respectively. CerS2 and CerS6 antibodies were diluted 1:200 and incubated over night, while the HSP90 antibody was diluted 1:1000 and incubated for 90 min. After washing, the blots were incubated with IRDye 680 conjugated goat anti-rabbit IgG(H + L) or IRDye 800CW conjugated goat anti-mouse IgG(H + L) secondary antibodies purchased from LI-COR (Bad Homburg, Germany). Membranes were analyzed on the Odyssey infrared scanner from LI-COR (Bad Homburg, Germany).

2.5. Silencing of CerS with siRNA

2.5×10^5 HCT-116 cells were transfected with 100 pmol CerS2 siRNA/CerS4 siRNA/CerS5 siRNA, 150 pmol CerS6 siRNA or 100 pmol scrambled siRNA as control. siPort Amine (Ambion, Darmstadt, Germany) was used for transfection according to the manufacturer's protocol. Briefly, Opti-MEM medium with transfection reagent was incubated for 10 min at RT, than added to the siRNA solution consisting of Opti-MEM medium and siRNA, followed by an incubation for 10 min at RT. 2.5×10^5 HCT-116 cells were incubated with siRNA transfection solution, and the process was repeated after 24 h. After 41 h the transfected HCT-116 cells were either harvested for mRNA isolation (RNA isolation kit (Qiagen, Hilden, Germany)) or treated with DMSO or 50 μM celecoxib and subjected to sphingolipid analysis. The effectiveness of the siRNA knock-down was verified using quantitative PCR.

2.6. Nude mice experiment

In a previous study we demonstrated that celecoxib exhibit also *in vivo* its antiproliferative effects using the nude mouse model [21]. For the current study brain, heart, lung, liver, small intestine, large intestine, kidney, testes and tumor tissue from these mice were extracted and washed with 0.9% saline and frozen by −80 °C. In all experiments, the ethics guidelines for investigations in conscious animals were obeyed and the local Ethics Committee for Animal Research approved the experiments.

2.7. In vitro cell viability assay

The WST-1 assay (Roche Diagnostic GmbH, Mannheim) was used to determine the viability and proliferation rate of the cells after treatment with CerS6 siRNA and celecoxib or DMSO. The cells were treated with 62.5 nMol CerS6 siRNA or 62.5 nMol scrambled siRNA for 41 h. Subsequently, the cells were treated either with 50 μM celecoxib or DMSO. After 20 h of incubation 10 μl of WST-1 reagent were added to each well and the cells were incubated for further 90 min. The formation of the dye was measured at 450 nm

against a reference wavelength of 620 nm using a 96-well spectrophotometric plate reader (SPECTRAFlour Plus, Tecan, Crailsheim, Germany). For the calculation of the cell viability the DMSO-treated cells were used as the 100% value.

2.8. Statistics

Ceramide levels, palmitoyl-CoA levels and mRNA expression data are presented as a mean ± S.E.M. (standard error of the mean). Ceramide data and mRNA expression data of the cell culture experiments were analyzed using an independent *t*-test and the confidence interval was set at 95%. Ceramide data of the nude mice experiments were analyzed using an independent *t*-test and the confidence interval was set at 95%, while the variances were assumed as not equal. The SPSS 9.01 software was used for statistical analyses.

3. Results

3.1. Time dependent alteration of ceramide levels in HCT-116 cells after treatment with celecoxib

We recently published that celecoxib inhibits the (dihydro)ceramide desaturase causing an increase of $C_{16:0}$-, $C_{24:1}$-, $C_{24:0}$-dihydroceramide and a decrease of $C_{24:1}$- and $C_{24:0}$-ceramide. Interestingly, the amount of $C_{16:0}$-ceramide remained unaltered in that study after 2 h of celecoxib (80 μM) treatment. However, the total ceramide level (includes $C_{16:0}$-, $C_{24:1}$-, $C_{24:0}$-dihydroceramide and ceramides) doubled relative to the control [18]. In this former study, we investigated shorter time periods with higher celecoxib concentrations (80 μM) since celecoxib exhibits an IC_{50} value of 79 ± 2 μM for the (dihydro)ceramide desaturase. For the present study, a concentration of 50 μM celecoxib was applied to minimize the influence of (dihydro)ceramide desaturase inhibition by celecoxib. Since the present study focused on the mechanism of sphingolipid pathway induction by celecoxib, HCT-116 cells were treated in a time dependent fashion up to 20 h with 50 μM celecoxib or DMSO (vehicle control). Ceramide concentrations were determined by LC–MS/MS. The treatment of HCT-116 cells with celecoxib time-dependently and significantly increased the amounts of $C_{16:0}$-dhCer, $C_{24:1}$-dhCer, $C_{24:0}$-dhCer, sphinganine and sphingosine as well as $C_{14:0}$-Cer, $C_{16:0}$-Cer and $C_{18:0}$-Cer (Fig. 1B, data are only partly shown). Instead, the ceramides $C_{20:0}$-, $C_{24:1}$- and $C_{24:0}$-ceramide decreased time-dependently (Fig. 1B). All in all, the total ceramide levels (including dihydroceramides ($C_{16:0}$-$C_{24:0}$), ceramides ($C_{14:0}$-$C_{24:0}$), sphingosine, sphinganine) increased by up to 210 ± 30% after incubation with 50 μM celecoxib for 6 h as compared to cells treated with DMSO.

3.2. mRNA and protein expression of CerSs and SPT in HCT-116 cells after celecoxib treatment

The observed increase of $C_{14:0}$-Cer, $C_{16:0}$-Cer and $C_{18:0}$-Cer could may be a consequence of induction of the key enzymes of the sphingolipid pathway CerSs and/or SPT (Fig. 1A). Therefore, we analyzed the expression level of CerSs and SPT by quantitative real time PCR and by western blot analysis. In HCT-116 cells, CerS2 may be the predominant isoform while CerS4, CerS5 and CerS6 are 6-fold less expressed (Fig. 2A). Experimentally, the expression level of CerS1 and CerS3 was below the limit of detection (data not shown). HCT-116 cells were incubated either with 50 μM celecoxib or with DMSO (control) for the indicated time periods. Our data exhibit that the mRNA expression of CerS2, which is specific for the synthesis of longer ceramides like $C_{24:1}$- and $C_{24:0}$-Cer (see Fig. 5B and Ref. [4]), significantly increased after celecoxib treatment whereas the expression levels of CerS4, CerS5 did not change. mRNA levels of CerS6 and SPTLC2 slightly but significantly

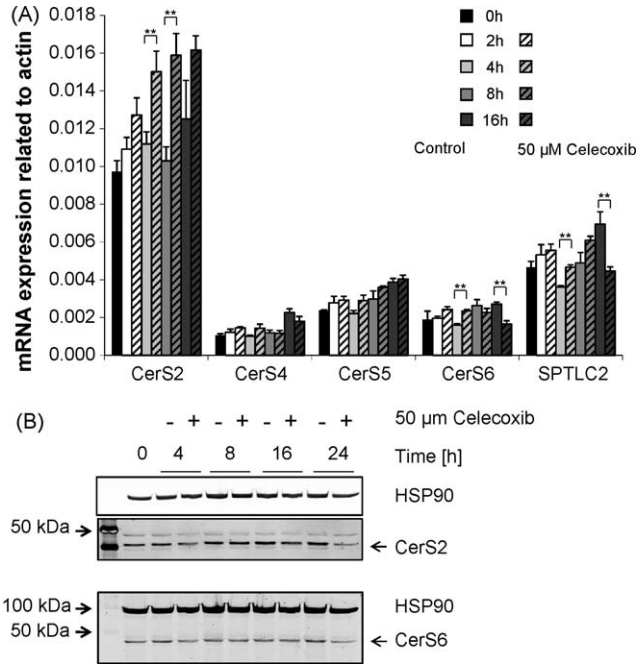

Fig. 2. The time-dependent effect of celecoxib both on the mRNA expression level and on the protein level of ceramide synthases. HCT-116 cells were treated for various time points as indicated with 50 μM celecoxib or with DMSO (control). (A) The relative mRNA expression of CerS2, CerS4, CerS5, CerS6 and SPTLC2 was normalized to β-actin. The relative mRNA levels were calculated with respect to control cells at the same time point. Data are mean ± S.E.M. of one of two comparable independent experiments, each achieved in duplicate. (B) Western blot analysis of CerS2 and CerS6. As internal standard the heat shock protein HSP90 was used (one of two independent experiments is shown).

increased after 4 h and decreased after 16 h of treatment with celecoxib as compared to the respective control. These results are unexpected due to the literature reports [4] and our own CerS6 knock-down experiments (see Fig. 5B) indicating that CerS6 is specific for the synthesis of short ceramides like $C_{16:0}$-Cer. Since the mRNA levels of CerS2 and CerS6 are slightly increased after celecoxib treatment, we checked the influence of celecoxib on protein levels of CerS2 and CerS6. HCT-116 cells were time-dependently incubated with 50 μM celecoxib or with DMSO (control). As shown in Fig. 2B celecoxib has no influence on the protein amounts of CerS2 or CerS6.

3.3. Ceramide synthase activity

As the increase of $C_{16:0}$-Cer after celecoxib treatment was most pronounced we focused in the following on this ceramide species. Our RNA and protein data suppose that the increase in $C_{16:0}$-Cer is not to be due to an upregulation of CerS6, therefore we investigated the ability of celecoxib to activate CerSs. Unfortunately, an activity assay using the microsomal fraction of HCT-116 cells showed no activation of CerSs by celecoxib treatment [18]. The same experiments also revealed that inhibition of the (dihydro)ceramide desaturase after celecoxib treatment was only detectable in living cells. Therefore, we developed a cell-based assay to detect the influence of celecoxib on ceramide synthase activity. In this assay, exogenously added sphingosine(C_{17}) functioned as substrate that is transformed to ceramides(C_{17}) by the action of the various ceramide synthases. The usage of sphingosine effectively excludes the participation of (dihydro)ceramide desaturase, which is responsible for the generation of ceramide from dihydroceramide if sphinganine (dihydro-sphingosine) is the substrate (see Fig. 1A). With the use of sphingosine(C_{17}), leading to the formation of ceramide(C_{17}), we could

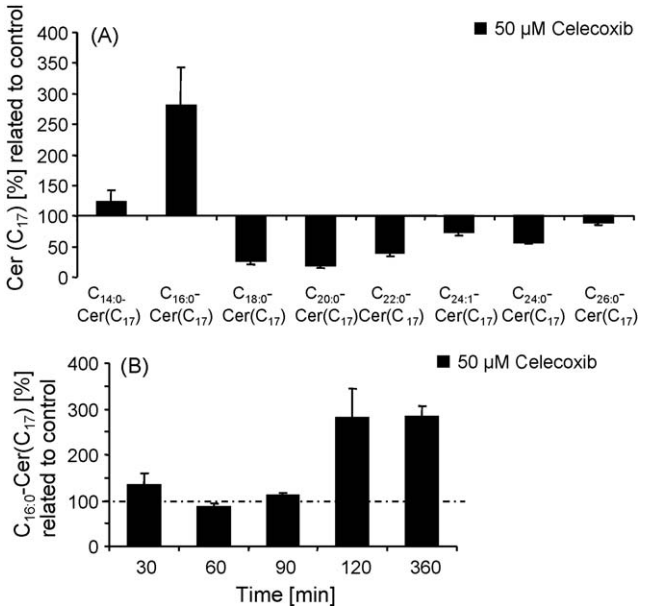

Fig. 3. Cell-based ceramide synthase activity assay. HCT-116 cells were preincubated for 90 min with 150 nM myriocin and than co-treated either with 50 µM celecoxib/5 µM sphingosine(C_{17})/150 nM myriocin or with DMSO/5 µM sphingosine(C_{17})/150 nM myriocin (control) for 2 h (A) or various time points (B). The amounts of ceramide(C17) were determined by LC–MS/MS. For analysis the area under the peak of the analyte was related to the area under the peak of the internal standard. The relative increase of the specific ceramides was calculated using the ratio analyte to internal standard of untreated cells as 100% value. The ceramide ratios were normalized to the number of treated cells. Data are mean ± S.E.M. of one of three comparable independent experiments each achieved in duplicate.

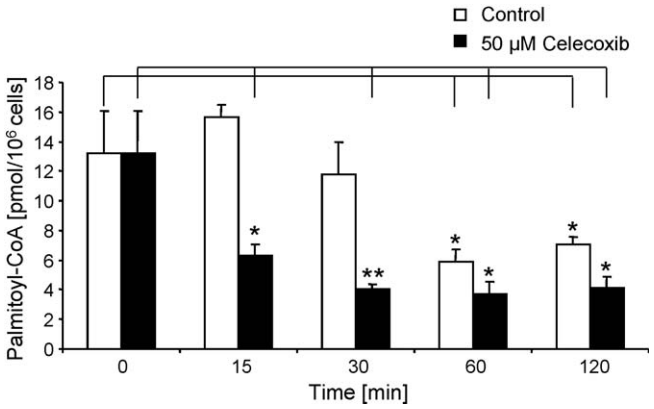

Fig. 4. Celecoxib treatment reduces the palmitoyl-CoA level in HCT-116 cells. HCT-116 cells were treated either with DMSO (white bars) or with 50 µM celecoxib (black bars) for the indicated time points. The palmitoyl-CoA levels were determined with LC–MS/MS and normalized to the number of treated cells. Data are mean ± S.E.M. of one of two comparable independent experiments each achieved in triplicate. $^{*}p < 0.05$ and $^{**}p < 0.01$ indicate significant difference between celecoxib and DMSO-treated cells at various time points and untreated cells (time point 0 h).

discriminate between endogenous ceramide(C_{18}) and the newly synthesized ceramide(C_{17}). Furthermore, HCT-116 cells were incubated with 150 nM myriocin, an inhibitor of the SPT, to block the endogenous sphinganine synthesis to reduce the natural substrate of the CerSs [18]. Inhibition of SPT does not influence the amounts of palmitoyl-CoA, a precursor of *de novo* sphingolipid synthesis (data not shown). HCT-116 cells were either incubated for 2 h with DMSO/5 µM sphingosine(C_{17})/150 nM myriocin (control) or with 50 µM celecoxib/5 µM sphingosine(C_{17})/150 nM myriocin (Fig. 3A). Following the incubation, sphingolipids were extracted and measured by LC–MS/MS. The levels of the different ceramide(C_{17}) species in control cells were set at 100%. The amounts of ceramide(C_{17}) species in cells treated with celecoxib were scaled to the control levels. Celecoxib treatment led to an increase of $C_{16:0}$-Cer(C_{17}) by 280%, and of $C_{14:0}$-Cer(C_{17}) by 123%, while the other ceramides ($C_{18:0}$-Cer(C_{17}), $C_{20:0}$-Cer(C_{17}), $C_{22:0}$-Cer(C_{17}), $C_{24:1}$-Cer(C_{17}), $C_{24:0}$-Cer(C_{17}), $C_{26:0}$-Cer(C_{17})) decreased. The increase of $C_{16:0}$-Cer occurs time-dependently and starts after treatment of cells with celecoxib for 2 h (Fig. 3B).

3.4. Celecoxib did not increase the palmitoyl-CoA level

Palmitoyl-CoA, in addition to sphingosine, is essential for the synthesis of $C_{16:0}$-Cer by the (dihydro)ceramide synthase. Addition of exogenous palmitoyl-CoA predominantly led to an increase of $C_{16:0}$-Cer (data not shown). To investigate whether or not celecoxib treatment leads to an increase of palmitoyl-CoA, which could in turn activate the (dihydro)ceramide synthase, we measured the amount of palmitoyl-CoA in celecoxib-treated HCT-116 cells using LC–MS/MS. As shown in Fig. 4, palmitoyl-CoA amounts time-dependently decreased within 2 h. The decrease was more pronounced in cells treated with 50 µM celecoxib than in control cells. The decrease of palmitoyl-CoA in untreated and celecoxib-treated cells could be due to an increase of ceramides (data not shown) induced either by celecoxib (see above) or by growth activation due to growth factors in fresh media.

3.5. Ceramide synthase 6 is involved in $C_{16:0}$-Cer synthesis in HCT-116 cells

Subsequently, we addressed the question whether or not celecoxib activates a specific CerS in HCT-116 cells. Therefore, we performed silencing experiments using siRNA for CerS2, CerS4, CerS5, and CerS6. HCT-116 cells were either untreated (control) or treated with scrambled siRNA, or the respective siRNAs for the various CerSs for 41 h. The mRNA expression was determined using relative quantitative PCR. The mRNA expression of the various CerSs was normalized to GAPDH and scaled to untreated cells. Scrambled siRNA (unspecific siRNA) led to a slight increase of the expression of all ceramide synthases as compared to untreated cells (Fig. 5A). The mRNA expression of CerS2, CerS4, CerS5 and CerS6 was reduced to 13%, 25%, 32%, 27%, respectively, by their specific siRNAs (Fig. 5A). The various siRNAs were specific, as demonstrated by the lack of significant cross-regulation to other CerSs (data not shown). Furthermore, none of the various siRNAs altered the mRNA expression of β-actin which was used as control (Fig. 5A). These results confirm the specificity of the CerS siRNAs to down-regulate their specific endogenous targets. To determine whether or not decreased mRNA expression levels affect the ceramide levels, we measured the ceramide levels after 41 h treatment with the various siRNAs. Silencing of CerS2 decreased the synthesis of $C_{24:1}$-Cer/$C_{24:0}$-Cer, silencing of CerS4 slightly decreased the synthesis of $C_{16:0}$-Cer/$C_{24:1}$-Cer/$C_{24:0}$-Cer and silencing of CerS6 significantly decreased the synthesis of $C_{16:0}$-Cer. Silencing of CerS5 had no effect on the predominantly synthesized ceramides (Fig. 5B). These data indicate that CerS6 is predominantly responsible for the synthesis of $C_{16:0}$-Cer. Therefore, we investigated, whether or not silencing of CerS6 by siRNA could also prevent the induction of $C_{16:0}$-Cer production in HCT-116 cells after celecoxib treatment. HCT-116 cells were pretreated with siRNA against CerS6. Afterwards, the cells were incubated with 150 nM myriocin, to inhibit sphingolipid *de novo* synthesis, and with DMSO/5 µM sphingosine(C_{17}) or 50 µM celecoxib/5 µM sphingosine(C_{17}) for 2 h. Treatment of cells with siRNA against CerS6 completely prevented the celecoxib-induced increase of $C_{16:0}$-Cer($_{17}$) in HCT-116 cells (Fig. 5C). In contrast, CerS2, CerS4 and CerS5 silencing in HCT-116 cells exhibited only a slight

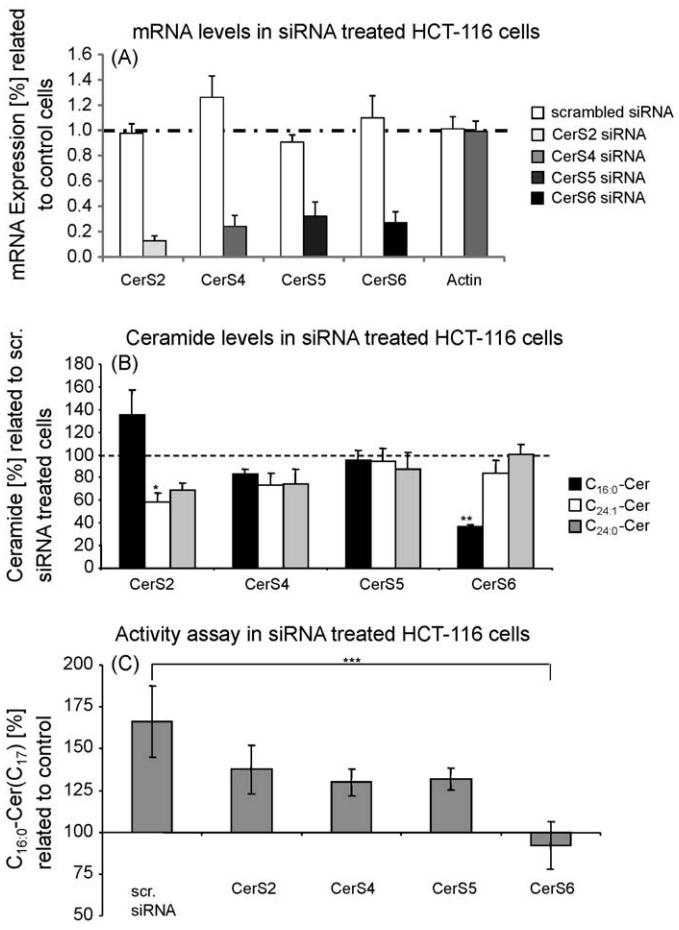

Fig. 5. Silencing of CerSs in HCT-116 cells using specific siRNAs. (A) mRNA level in siRNA treated HCT-116 cells. The cells were incubated for 41 h with CerS2, CerS4, CerS5, CerS6 or scrambled siRNA. The mRNA expression of CerS2, CerS4, CerS5 and CerS6 was normalized to GAPDH. The relative mRNA expressions of the CerSs were calculated using cells treated only with transfection reagent as 100% value. As an additional control for the specificity of the siRNA treatment we checked the mRNA expression of β-actin. As a representative experiment the mRNA expression of β-actin after treatment with CerS4 siRNA is indicated. Data are mean ± S.E.M. of three independent experiments each achieved in triplicate. (B) Ceramide levels in siRNA (scrambled, CerS2, CerS4, CerS5, CerS6) treated HCT-116 cells. The ceramide levels were determined using LC–MS/MS and were normalized to the number of treated cells. The relative ceramide level was calculated using the ceramide level of HCT-116 cells treated with scrambled siRNA as 100% value. Data are mean ± S.E.M. of two independent experiments each achieved in duplicate. $^{**}p < 0.01$ and $^{*}p < 0.05$ indicate significant difference between CerS siRNA treated and scrambled siRNA treated cells. (C) Activity assay in siRNA treated HCT-116 cells. After 41 h treatment with siRNA (against CerS2, CerS4, CerS5, CerS6 or scrambled) HCT-116 cells were preincubated 90 min with 150 nM myriocin and subsequently co-incubated with 50 μM celecoxib/5 μM sphingosine(C_{17})/150 nM myriocin or with DMSO/5 μM sphingosine(C_{17})/150 nM myriocin (control) for 2 h. The amounts of ceramide(C_{17}) were determined by LC–MS/MS. For analysis the area under the peak of the analyte was related to the area under the peak of the internal standard. The relative increase of the specific ceramides was calculated using the ratio analyte to internal standard of DMSO-treated cells as 100% value. The ceramide ratios were normalized to the number of treated cells. Data are mean ± S.E.M. of one of three comparable independent experiments each achieved in duplicate. $^{***}p < 0.001$ indicates significant difference between celecoxib-treated and control cells.

decrease in $C_{16:0}$-Cer(C_{17}) synthesis induced by celecoxib. In conclusion both the cell-based activity assay as well as the ceramide expression pattern after silencing various CerSs points to CerS6 as a target of celecoxib.

3.6. Celecoxib activates the salvage pathway

Ceramides are either synthesized via a salvage pathway or *de novo* synthesis. Since ceramide synthases play an essential role in both pathways, we investigated which pathway is activated by celecoxib. For this purpose, an inhibitor of the L-serine palmitoyl transferase (myriocin) was used, which only blocks the *de novo* synthesis. In contrast, the non-selective ceramide synthase inhibitor fumonisin B1 (FB1) blocks both the salvage pathway and the *de novo* synthesis of ceramides. HCT-116 cells were incubated with either DMSO (control), 50 μM celecoxib, 70 μM FB1, 150 nM myriocin or co-treated with a mixture of 50 μM celecoxib/70 μM FB1 or 50 μM celecoxib/150 nM myriocin for 6 h. In Fig. 6A we were able to show that myriocin alone reduces the $C_{16:0}$-Cer levels below the control levels (dark grey bar). In comparison, treatment of cells with 50 μM celecoxib and myriocin (striped, dark grey bar) reduces the ceramide levels approximately to control (white bar), but as compared to the myriocin treated cells (dark grey bar), the inhibition is not complete. Instead, fumonisin B1 inhibits ceramide production nearly to the same extend in control cells as well as in celecoxib-treated cells. The difference in $C_{16:0}$-Cer levels between celecoxib/fumonisin B1 treated cells and cells treated with celecoxib/myriocin may be due to the ceramide synthesized by the salvage pathway. Desipramine induces the degradation of the acid sphingomyelinase and the down-regulation of acid ceramidase [22] leading to a partial inhibition of the salvage pathway (Fig. 1A). HCT-116 cells were incubated with either DMSO (control), 50 μM celecoxib, 20 μM desipramine or co-treated with a mixture of 50 μM celecoxib/20 μM desipramine 6 h. Fig. 6C shows that treatment of control cells with desipramine alone has only a slight effect on $C_{16:0}$-Cer levels, indicating that the sphingomyelinase pathway plays only a minor role for the synthesis of $C_{16:0}$-Cer in control cells. In contrast, desipramine completely prevents the increase of ceramide induced by celecoxib treatment. These data point out that after celecoxib treatment the *de novo* synthesis plays only a minor role for the production of $C_{16:0}$-Cer whereas the salvage pathway seems to have a more important role. Treatment of HCT-116 cells with celecoxib significantly increased the amount of sphingosine, which is a key precursor of the salvage pathway (see Figs. 1A and 6B). 20 μM desipramine reduced the sphingosine level in control cells and completely prevented an increase of sphingosine after celecoxib treatment (Fig. 6B). These data indicate that celecoxib treatment leads to an activation of the salvage pathway in HCT-116 cells.

3.7. Celecoxib specifically increases $C_{16:0}$-Cer in nude mice tissue

In order to support the results obtained *in vitro*, nude mice were used to generate *in vivo* data. We demonstrated in a previous study that celecoxib inhibits the tumor growth of HCT-116 xenografts in nude mice [21]. Nude mice were treated for 3 weeks with 10 mg/kg celecoxib or with vehicle. For further analysis, the brain, lung, heart, stomach, large intestine, small intestine, testes and the tumor tissues were extracted. The tissues were homogenized and the sphingolipids were extracted and determined by LC–MS/MS. In line with the *in vitro* data, celecoxib treatment significantly increased the level of $C_{16:0}$-Cer in stomach, small intestine and tumor tissue of the nude mice (Fig. 7). No differences were detectable in the other tissues investigated. Interestingly, no changes were observed after celecoxib treatment for $C_{24:1}$-Cer and $C_{24:0}$-Cer.

3.8. Silencing of CerS6 protects cells against the antiproliferative effect of celecoxib

Next we checked, whether the increased $C_{16:0}$-Cer level could be at least in part responsible for the observed toxic effects of celecoxib. For this purpose we silenced the CerS6 expression transiently in HCT-116 cells and compared the toxic effects of celecoxib with control HCT-116 cells. Treatment of HCT-116 cells with 50 μM celecoxib for 24 h reduced the viability of control cells

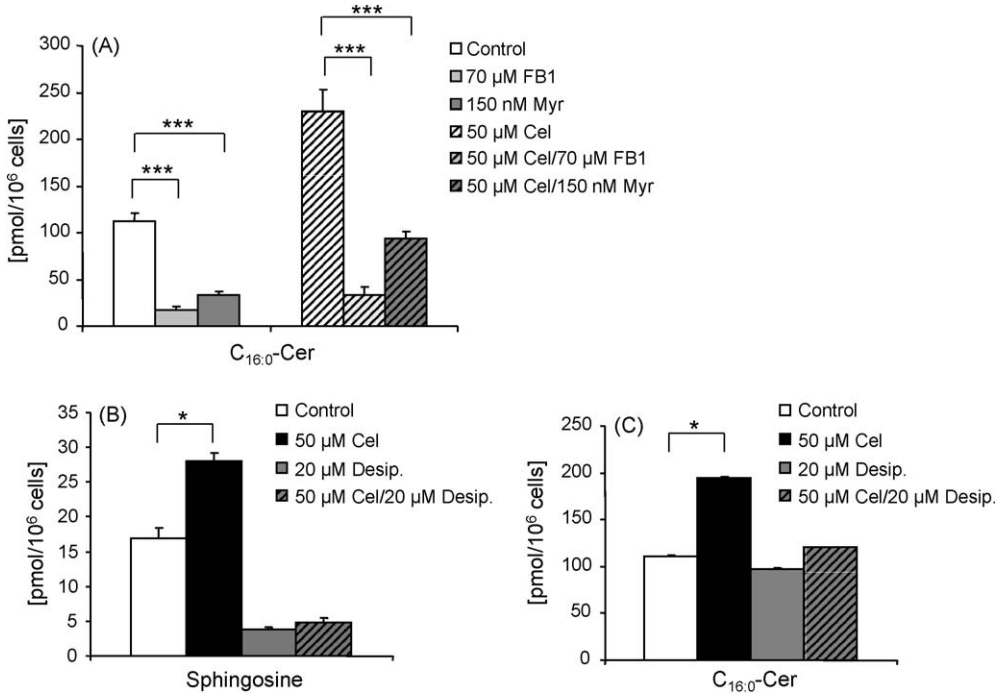

Fig. 6. (A) $C_{16:0}$-Cer level in HCT-116 cells after treatment with celecoxib and inhibitors of the *de novo* synthesis or salvage pathway. HCT-116 cells were preincubated (90 min) with 70 μM FB1, 150 nM myriocin or DMSO and subsequently treated with DMSO (control), 50 μM celecoxib, 70 μM FB1, 50 μM celecoxib/70 μM FB1, 150 nM myriocin, 150 nM myriocin/50 μM celecoxib for 6 h. (B and C) The sphingosine (B) and $C_{16:0}$-Cer (C) level in HCT-116 cells after treatment with celecoxib and desipramine. HCT-116 cells were preincubated (90 min) with 20 μM desipramine or DMSO and subsequently treated with DMSO (control), 50 μM celecoxib, 20 μM desipramine and 50 μM celecoxib/20 μM desipramine for 6 h. The $C_{16:0}$-Cer and sphingosine levels determined with LC–MS/MS were normalized to the number of treated cells. Data are mean ± S.E.M. of two independent experiments each achieved in duplicate. A significant increase of $C_{16:0}$-Cer and sphingosine as indicated are marked with an asterisk ($^*p < 0.05$ and $^{***}p < 0.001$). *Abbreviations*: Cel, celecoxib; FB1, fumonisin B1; Myr, myriocin, Desip, desipramine.

about 24% and only about 8% in CerS6 silenced cells (Fig. 8). These data indicate that activation of CerS6 and therefore an increase in $C_{16:0}$Cer is important for the toxic effect of celecoxib.

4. Discussion

Investigations about the "specialization" of ceramides, especially their specific synthesis and their sophisticated role in cell regulation are currently a hot topic of research. To date, few reports describe the differential regulation of ceramides with various chain lengths. As data accumulate, it is becoming increasingly apparent that the chain length, subcellular location and the biosynthetic pathway (salvage or *de novo*) of ceramides all contribute to physiological and pathophysiological regulatory mechanisms in the cell [11]. Moreover, there are various proteins that can recognize ceramides with a high degree of fatty acid chain length specificity, such as the ceramide transport protein CERT (preference for $C_{16:0}$-Cer/$C_{18:0}$-Cer) [23] and the inhibitor 2 of protein phosphatase2A (preference for $C_{18:0}$-Cer) [24].

Celecoxib induces a significant increase of $C_{16:0}$-Cer *in vitro* in HCT-116 colon carcinoma cells as well as *in vivo* in nude mouse tissues, the stomach, the small intestine and tumor tissues. This elevation was attributed to an elevated enzymatic activity of CerS6 and not to transcriptional upregulation of CerS6. In another study we could show that only the overexpression of CerS6 in HCT-116 cells led to an increase of $C_{16:0}$-Cer (unpublished data). Furthermore, we demonstrated that celecoxib activates predominantly the salvage pathway, as inhibition of the *de novo* synthesis by L-serine palmitoyl transferase inhibitor only slightly prevents the increase of $C_{16:0}$-Cer amounts, while inhibition of CerSs by fumonisin B1 blocks more effective the increase of $C_{16:0}$-Cer amounts. Apart from inhibiting N-acylation of sphinganine, which occurs downstream of the SPT, fumonisin B1 also blocks the reacylation of sphingosine produced by the salvage pathway (see also Fig. 1A). Nevertheless, both, the increase of the mRNA level of SPT and of sphinganine followed by treatment with celecoxib as well as the effectiveness of myriocin suggest that also the *de novo* synthesis is involved. Interestingly, the endocannabinoid analog R(+)-methanandamide increased the ceramide level in neuroglioma cells by activating the ceramide synthases of the salvage pathway but not of *de novo* synthesis, since the ceramide upregulation was prevented by fumonisin B1 but not by myriocin [25]. Furthermore, desipramine, blocking the degradation of sphingomyeline to ceramide by aSMase, which is one resource of sphingosine, completely prevented the increase of sphingosine and $C_{16:0}$-Cer after celecoxib treatment.

In a previous study we could show that myriocin prevents, at least partially, celecoxib-induced growth inhibition as well as apoptosis [18]. With the data presented here, we could demonstrate that the salvage pathway and CerS6 are targets of celecoxib. Silencing of CerS6 significantly reduced celecoxib-induced growth inhibition (Fig. 8), suggesting that specific activation of this ceramide synthase and thereby accumulation of $C_{16:0}$-Cer contributes to the toxic effects of celecoxib. The role of $C_{16:0}$-Cer and other ceramides in cancer development is actually highly debated. In this regard White-Gilbertson et al. reported that TRAIL-(tumor necrosis factor-related apoptosis-inducing ligand-) induced apoptosis depends on activation of CerS6 and synthesis of $C_{16:0}$-Cer [26]. Moreover, irradiation treatment of Molt-4 leukemia cells led to a p53 dependent synthesis of $C_{16:0}$-Cer through a transcriptional upregulation of CerS5 [27]. Furthermore not only the increase or decrease of one specific ceramide could be involved in tumor development but also an altered ratio of the ceramides. Liu et al. [28] postulated that the altered ratio of $C_{16:0}$-Cer/$C_{24:0}$-Cer is responsible for the induction of apoptosis. The observation that an increase in the ratio of $C_{16:0}$-Cer/$C_{24:0}$-Cer from 1.28 in untreated

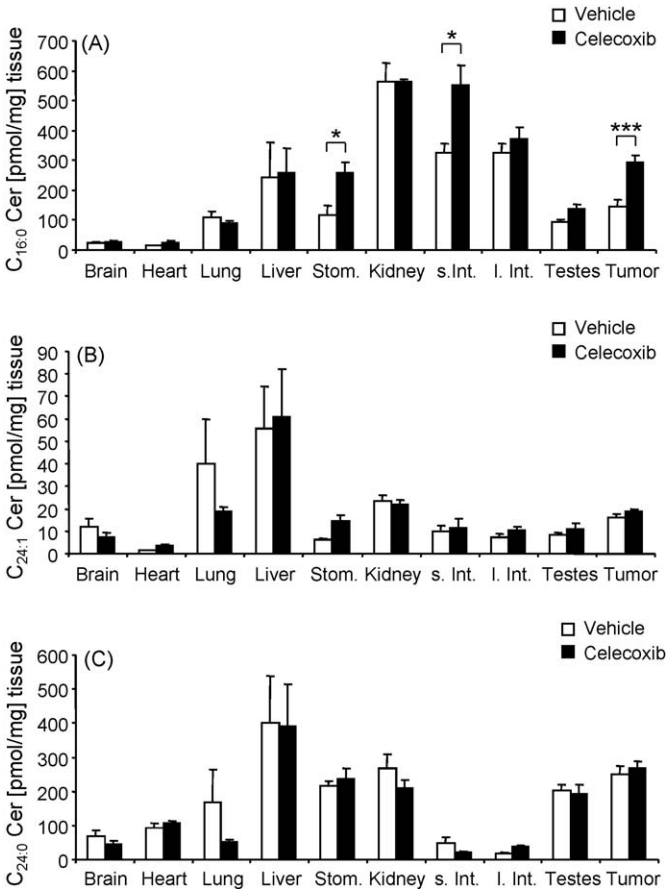

Fig. 7. Effects of orally administered celecoxib on the $C_{16:0}$-Cer (A), $C_{24:1}$-Cer (B) and $C_{24:0}$-Cer (C) ceramide level in mouse tissue. Approximately 1×10^7 HCT-116 tumor cells were injected subcutaneously into the left and right dorsal flank of nude mice. Mice received either vehicle or 10 mg/kg celecoxib daily. Treatment started 4 days post implantation. After 3 weeks the mice were sacrificed, the tissues (brain, heart, lung, liver, stomach (stom.), kidney, small intestine (s. int.), large intestine (l. int.), testis, tumor) were extracted, washed with 0.9% saline and the amount of ceramides were determined using LC–MS/MS. A significant increase of ceramide amount in celecoxib-treated mice versus untreated control mice is indicated with an asterisk ($^*p < 0.05$ and $^{***}p < 0.001$).

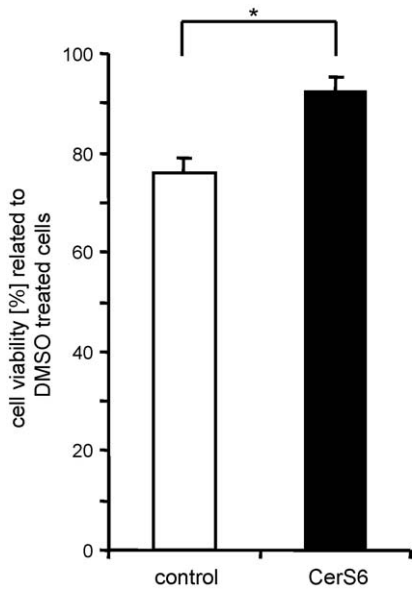

Fig. 8. Effect of CerS6 silencing on celecoxib-induced cell toxicity. HCT-116 cells were pretreated with 62.5 nMol CerS6 siRNA or with 62.5 nMol scrambled siRNA (control) for 41 h and subsequently treated either with 50 μM celecoxib or with DMSO for 20 h. Cell viability was determined using the WST-1 proliferation assay. Data are mean ± S.E.M. of one of three comparable independent experiments each achieved in duplicate. $^*p < 0.01$ indicates significant difference between scrambled siRNA and CerS6 siRNA treated cells.

cells to 3.09 in celecoxib-treated (50 μM, 6 h) cells supports the notion that the ratio $C_{16:0}$-Cer/$C_{24:0}$-Cer is critical.

But our data raises another important question: how does celecoxib selectively activate one specific ceramide synthase? Ceramide synthases are located at the endoplasmic reticulum, where the *de novo* synthesis occurs [29] and at mitochondria-associated membranes [30]. However, whether these enzymes are also involved in *de novo* synthesis or whether they only play a role in the salvage pathway is not clear. Interestingly, a previous study revealed that during cerebral ischemia/reperfusion mitochondrial ceramide levels are elevated due to the activation of mitochondrial ceramide synthases by post-translational mechanisms [31]. Interestingly, in mouse brain only CerS1, CerS2 and CerS6 are located in the mitochondrial membrane, while CerS5 is located in the endoplasmic reticulum [31]. Such specific localizations could be the rationale for the specific activation of CerS6 in HCT-116 cells by celecoxib. The activation of CerS6 after celecoxib treatment is only observable in living cells with intact membrane structures. Recently, we showed that celecoxib accumulates specifically in cellular membranes [32]. This accumulation of celecoxib may explain why we only observed an activation of CerS6 in viable cells. Furthermore, activation of an enzyme may depend on post-translational modifications as well as co-factor and substrate availability. An increase in substrate availability could be excluded in these experiments, because celecoxib does not raise the palmitoyl-CoA concentration. Beside of a direct mechanism, several possibilities for an indirect activation exist: (1) *Alterations in the quaternary structure of the CerSs*. Koyanagi et al. linked already augmented levels of dihydroceramide and ceramide in tumor tissue to CerSs with a larger than normal molecular mass [33]. (2) *Translocation processes of the CerSs*. Cisplatin induces rapid translocation of CerS1 but not CerS4 or CerS5 from ER to Golgi apparatus [7]. (3) *Phosphorylation of the CerSs*. Using the SWISS_Prot data bank we found several potential phosphorylation sides in the CerS6 protein sequence. But whether one of these mechanisms contributes to the effect observed after celecoxib treatment requires further investigations.

In conclusion, our data clearly demonstrate that celecoxib activates CerS6 and thereby causes an increase of $C_{16:0}$-Cer level, which, in turn, contributes to the toxic effects of celecoxib. The influence of celecoxib on the sphingolipid pathway might be of great clinical relevance. On the one hand celecoxib is used in clinical trials for cancer treatment regimes. On the other hand celecoxib is investigated for usability against Alzheimer disease [34]. Progression of this disease is positively correlated with ceramide levels [35].

Acknowledgements

The authors thank Dr. Wesley McGinn-Straub for the linguistic revision of the manuscript. This work was supported by the Deutsche Forschungsgemeinschaft (DFG) Forschergruppe FOG 784/TP5 (GR2011/2-1) and the LOEWE Lipid Signaling Forschungszentrum Frankfurt (LiFF).

References

[1] Ogretmen B, Hannun YA. Biologically active sphingolipids in cancer pathogenesis and treatment. Nat Rev Cancer 2004;4(8):604–16.
[2] Pewzner-Jung Y, Ben-Dor S, Futerman AH. When do Lasses (longevity assurance genes) become CerS (ceramide synthases)?: insights into the regulation of ceramide synthesis. J Biol Chem 2006;281(35):25001–5.

[3] Rabionet M, van der Spoel AC, Chuang CC, von Tumpling-Radosta B, Litjens M, Bouwmeester D, et al. Male germ cells require polyenoic sphingolipids with complex glycosylation for completion of meiosis: a link to ceramide synthase-3. J Biol Chem 2008;283(19):13357–69.
[4] Mizutani Y, Kihara A, Igarashi Y. Mammalian Lass6 and its related family members regulate synthesis of specific ceramides. Biochem J 2005;390(Pt 1):263–71.
[5] Riebeling C, Allegood JC, Wang E, Merrill Jr AH, Futerman AH. Two mammalian longevity assurance gene (LAG1) family members, trh1 and trh4, regulate dihydroceramide synthesis using different fatty acyl-CoA donors. J Biol Chem 2003;278(44):43452–9.
[6] Laviad EL, Albee L, Pankova-Kholmyansky I, Epstein S, Park H, Merrill Jr AH, et al. Characterization of ceramide synthase 2: tissue distribution, substrate specificity, and inhibition by sphingosine 1-phosphate. J Biol Chem 2008;283(9):5677–84.
[7] Min J, Mesika A, Sivaguru M, Van Veldhoven PP, Alexander H, Futerman AH, et al. (Dihydro)ceramide synthase 1 regulated sensitivity to cisplatin is associated with the activation of p38 mitogen-activated protein kinase and is abrogated by sphingosine kinase 1. Mol Cancer Res 2007;5(8):801–12.
[8] Ruvolo PP. Intracellular signal transduction pathways activated by ceramide and its metabolites. Pharmacol Res 2003;47(5):383–92.
[9] Perry DK, Carton J, Shah AK, Meredith F, Uhlinger DJ, Hannun YA. Serine palmitoyltransferase regulates de novo ceramide generation during etoposide-induced apoptosis. J Biol Chem 2000;275(12):9078–84.
[10] Charles AG, Han TY, Liu YY, Hansen N, Giuliano AE, Cabot MC. Taxol-induced ceramide generation and apoptosis in human breast cancer cells. Cancer Chemother Pharmacol 2001;47(5):444–50.
[11] Modrak DE, Gold DV, Goldenberg DM. Sphingolipid targets in cancer therapy. Mol Cancer Ther 2006;5(2):200–8.
[12] Guenther GG, Peralta ER, Rosales KR, Wong SY, Siskind LJ, Edinger AL. Ceramide starves cells to death by downregulating nutrient transporter proteins. Proc Natl Acad Sci USA 2008;105(45):17402–7.
[13] Selzner M, Bielawska A, Morse MA, Rudiger HA, Sindram D, Hannun YA, et al. Induction of apoptotic cell death and prevention of tumor growth by ceramide analogues in metastatic human colon cancer. Cancer Res 2001;61(3):1233–40.
[14] Koki AT, Masferrer JL. Celecoxib: a specific COX-2 inhibitor with anticancer properties. Cancer Control 2002;9(2 Suppl.):28–35.
[15] Steinbach G, Lynch PM, Phillips RK, Wallace MH, Hawk E, Gordon GB, et al. The effect of celecoxib, a cyclooxygenase-2 inhibitor, in familial adenomatous polyposis. N Engl J Med 2000;342(26):1946–52.
[16] Grosch S, Maier TJ, Schiffmann S, Geisslinger G. Cyclooxygenase-2 (COX-2)-independent anticarcinogenic effects of selective COX-2 inhibitors. J Natl Cancer Inst 2006;98(11):736–47.
[17] Maier TJ, Tausch L, Hoernig M, Coste O, Schmidt R, Angioni C, et al. Celecoxib inhibits 5-lipoxygenase. Biochem Pharmacol 2008;76(7):862–72.
[18] Schiffmann S, Sandner J, Schmidt R, Birod K, Wobst I, Schmidt H, et al. The selective COX-2 inhibitor celecoxib modulates sphingolipid synthesis. J Lipid Res 2009;50(1):32–40.
[19] Brautigam L, Vetter G, Tegeder I, Heinkele G, Geisslinger G. Determination of celecoxib in human plasma and rat microdialysis samples by liquid chromatography tandem mass spectrometry. J Chromatogr B Biomed Sci Appl 2001;761(2):203–12.
[20] Schiffmann S, Sandner J, Birod K, Wobst I, Angioni C, Ruckhaberle E, et al. Ceramide synthases and ceramide levels are increased in breast cancer tissue. Carcinogenesis 2009;30(5):745–52.
[21] Schiffmann S, Maier TJ, Wobst I, Janssen A, Corban-Wilhelm H, Angioni C, et al. The anti-proliferative potency of celecoxib is not a class effect of coxibs. Biochem Pharmacol 2008;76(2):179–87.
[22] Elojeimy S, Holman DH, Liu X, El-Zawahry A, Villani M, Cheng JC, et al. New insights on the use of desipramine as an inhibitor for acid ceramidase. FEBS Lett 2006;580(19):4751–6.
[23] Kudo N, Kumagai K, Tomishige N, Yamaji T, Wakatsuki S, Nishijima M, et al. Structural basis for specific lipid recognition by CERT responsible for nonvesicular trafficking of ceramide. Proc Natl Acad Sci USA 2008;105(2):488–93.
[24] Mukhopadhyay A, Saddoughi SA, Song P, Sultan I, Ponnusamy S, Senkal CE, et al. Direct interaction between the inhibitor 2 and ceramide via sphingolipid-protein binding is involved in the regulation of protein phosphatase 2A activity and signaling. FASEB J 2008.
[25] Ramer R, Weinzierl U, Schwind B, Brune K, Hinz B. Ceramide is involved in r(+)-methanandamide-induced cyclooxygenase-2 expression in human neuroglioma cells. Mol Pharmacol 2003;64(5):1189–98.
[26] White-Gilbertson S, Mullen T, Senkal C, Lu P, Ogretmen B, Obeid L, et al. Ceramide synthase 6 modulates TRAIL sensitivity and nuclear translocation of active caspase-3 in colon cancer cells. Oncogene 2009;28(8):1132–41.
[27] Panjarian S, Kozhaya L, Arayssi S, Yehia M, Bielawski J, Bielawska A, et al. De novo N-palmitoylsphingosine synthesis is the major biochemical mechanism of ceramide accumulation following p53 up-regulation. Prostaglandins Other Lipid Mediat 2008;86(1–4):41–8.
[28] Liu X, Elojeimy S, Turner LS, Mahdy AE, Zeidan YH, Bielawska A, et al. Acid ceramidase inhibition: a novel target for cancer therapy. Front Biosci 2008;13:2293–8.
[29] Futerman AH, Riezman H. The ins and outs of sphingolipid synthesis. Trends Cell Biol 2005;15(6):312–8.
[30] Bionda C, Portoukalian J, Schmitt D, Rodriguez-Lafrasse C, Ardail D. Subcellular compartmentalization of ceramide metabolism: MAM (mitochondria-associated membrane) and/or mitochondria? Biochem J 2004;382(Pt 2):527–33.
[31] Yu J, Novgorodov SA, Chudakova D, Zhu H, Bielawska A, Bielawski J, et al. JNK3 signaling pathway activates ceramide synthase leading to mitochondrial dysfunction. J Biol Chem 2007;282(35):25940–9.
[32] Maier TJ, Schiffmann S, Wobst I, Birod K, Angioni C, Hoffmann M, et al. Cellular membranes function as a storage compartment for celecoxib. J Mol Med 2009.
[33] Koyanagi S, Kuga M, Soeda S, Hosoda Y, Yokomatsu T, Takechi H, et al. Elevation of de novo ceramide synthesis in tumor masses and the role of microsomal dihydroceramide synthase. Int J Cancer 2003;105(1):1–6.
[34] Group AR, Lyketsos CG, Breitner JC, Green RC, Martin BK, Meinert C, et al. Naproxen and celecoxib do not prevent AD in early results from a randomized controlled trial. Neurology 2007;68(21):1800–8.
[35] Katsel P, Li C, Haroutunian V. Gene expression alterations in the sphingolipid metabolism pathways during progression of dementia and Alzheimer's disease: a shift toward ceramide accumulation at the earliest recognizable stages of Alzheimer's disease? Neurochem Res 2007;32(4–5):845–56.